Williams, P. G. et al. Saliniketals A and B, Bicyclic Polyketides from the Marine Actinomycete Salinispora arenicola. J. Nat. Prod. 70, 83-88

ARTICLE *in* JOURNAL OF NATURAL PRODUCTS · FEBRUARY 2007

Impact Factor: 3.8 · DOI: 10.1021/np0604580 · Source: PubMed

Saliniketals A and B, Bicyclic Polyketides from the Marine Actinomycete *Salinispora arenicola*

Philip G. Williams,[†,§] Ratnakar N. Asolkar,[†] Tamara Kondratyuk,[‡] John M. Pezzuto,[‡,⊥] Paul R. Jensen,[†] and William Fenical*[,†]

Center for Marine Biotechnology and Biomedicine, Scripps Institution of Oceanography, University of California−San Diego, La Jolla, California 92093-0204, and Department of Medicinal Chemistry and Molecular Pharmacology, Purdue University, West Lafayette, Indiana 47907

Received September 18, 2006

An extensive study of the secondary metabolites produced by several strains of the marine actinomycete *Salinispora arenicola* has led to the isolation of two unusual bicyclic polyketides, saliniketals A and B (**1**, **2**). The structures, which contain a new 1,4-dimethyl-2,8-dioxabicyclo[3.2.1]octan-3-yl ring, were assigned mainly by 2D NMR spectroscopic methods. Unexpectedly, chemical derivatization of saliniketal A with Mosher's acid chloride resulted in a functional group interconversion of an unsaturated primary amide to the corresponding nitrile in a quantitative yield under unusually mild conditions. Saliniketals A and B were found to inhibit ornithine decarboxylase induction, an important target for the chemoprevention of cancer, with IC_{50} values of 1.95 ± 0.37 and 7.83 ± 1.2 μg/mL, respectively.

In the last 20 years, new treatments for advanced cancers have resulted in some improvements in mortality rates. Clearly, however, treatments are only partially effective, and a steady increase in the incident rates for skin, breast, and renal cancers remains of serious concern.[1] Carcinogenesis is generally believed to be the culmination of damage to numerous regulatory genes that ultimately results in the development of invasive and metastatic cancers.[2] This suggests that an alternative to the treatment of these cancers would be the prevention of damage to these regulatory genes. Advancements over the last few decades in understanding the molecular basis of cancer progression now make it viable to use natural products[3] or synthetic drugs to inhibit the development of cancer by blocking DNA damage or by arresting the development of premalignant cells that have already incurred damage. This strategy has been termed chemoprevention.

In the 1980s, genetic studies demonstrated that polyamines, organic cations derived from amino acids, are essential for the optimal growth and viability of bacteria[4] and yeast.[5] Subsequent studies showed that the enzyme responsible for the first step in polyamine biosynthesis, ornithine decarboxylase (ODC), was essential in mice, thus extending the importance of these organic cations to mammals. Studies on mice harboring a disrupted ODC gene showed that loss of ODC did not block normal development of embryo to the blastocyst stage. ODC-deficient embryos were capable of uterine implantation yet failed to develop thereafter. Therefore, ODC plays an essential role in murine development and proper homeostasis of polyamine pools appears to be required for cell survival.[6] It is now known that polyamines have an essential role in normal cellular proliferation and that ODC is downregulated as cells become senescent[7] in many adult tissues.[8] Furthermore, several groups have shown that ODC is a directed transcriptional target of the oncogene *MYC*[9,10] and is overexpressed in various tumor cells.[11] Thus, inhibiting ODC activity to decrease the cellular concentration of polyamines may represent an effective strategy to prevent carcinogenesis.[12−14] Studies with an irreversible inhibitor of ODC, α-difluoromethylornithine (α-DFMO), have validated this approach by demonstrating a decrease in cellular putrescine and spermidine levels and the inability of these cells to form tumors in severe combined immunodeficient mice.[15]

On the basis of this rationale, we began screening extracts of obligate marine actinomycetes for inhibitors of phorbol ester-induced ornithine decarboxylase. Herein, we report the isolation and structure determination of saliniketals A (**1**) and B (**2**), two ODC inhibitors with novel structures.

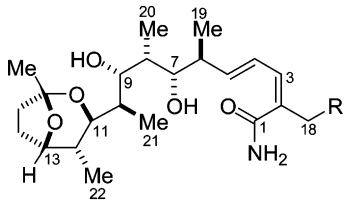

Saliniketal A (**1**) R = H
Saliniketal B (**2**) R= OH

Results and Discussion

Saliniketal A (**1**) was isolated as an optically active, amorphous powder ($[\alpha]_D^{24}$ −13.7, MeOH). The molecular formula of **1** was established as $C_{22}H_{37}NO_5$ on the basis of a pseudomolecular ion peak at 396.2760 ($[MH]^+$, error 2.5 ppm) that indicated **1** contained 5 degrees of unsaturation. Clearly, on the basis of the UV absorption at 240 nm, some of these double-bond equivalents could be attributed to a simple conjugated chromaphore. This conclusion was supported by signals in the proton NMR spectrum indicative of an α,*β*,*γ*,*δ*-unsaturated system (δ_H 6.17 br d, 6.60 dd, and 5.78 dd). This system was expanded at one end on the basis of HMBC correlations from H-3 (δ_H 6.17 br d) to an allylic methyl group (C-18), a quaternary sp^2 carbon (C-2), and a carbonyl carbon (Figure 1). Another three-carbon fragment was constructed through interpretation of HMBC correlations from a methyl doublet (H_3-20) to three methine carbons, two of which, C-7 and C-9, were clearly oxygenated due to their downfield carbon chemical shifts at δ_C 75.8 and 78.2, respectively. A suite of COSY correlations from H-9 to the methine proton H-10 and then from H-10 to the methyl doublet H_3-21 enlarged this small unit into a six-carbon fragment formally derived from the aldol condensation of two propionate units. This suggested that **1** was a polyketide. This knowledge facilitated the assembly of the final segment, as HMBC correlations from the remaining methyl doublet (H_3-22) constructed a 2-methyl-1,3-propandiol unit, which contained C-11 through C-13. An HMBC correlation from the proton of this latter carbon (H-13) to a quaternary carbon, which had a distinctive carbon chemical shift (δ_C 106.4 ppm) that was diagnostic of a ketal functional group, expanded this three-carbon unit. The downfield carbon signal, C-16,

* To whom correspondence should be addressed. Tel: (858) 534-2133. Fax: (858) 558-3702. E-mail: wfenical@ucsd.edu.
† Scripps Institution of Oceanography.
§ Current address: University of Hawaii at Manoa, Department of Chemistry, Honolulu, Hawaii 96822.
‡ Purdue University.
⊥ Current address: University of Hawaii at Hilo, College of Pharmacy, Hilo, Hawaii 96720.

10.1021/np0604580 CCC: $37.00
Published on Web 12/13/2006

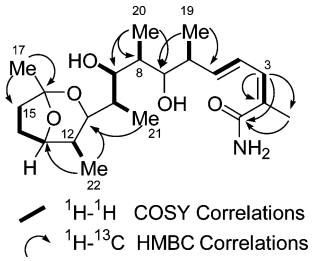

Figure 1. Key correlations used to construct **1**.

also showed HMBC correlations from an isolated methyl singlet H_3-17 and an envelope of proton signals at 1.90 ppm. The latter showed COSY cross-peaks to the pair of methylene proton signals H_2-15 and then back to H-13 to form a substituted tetrahydrofuran ring system.

The fundamental structure was then assembled from HMBC correlations between these three fragments. Specifically, an HMBC correlation between the methyl group H_3-21 and C-11 connected the second and third fragments at the C-10/C-11 juncture, while cross-peaks from the methyl group H_3-19 to C-7 and C-5 linked this larger moiety to the final fragment containing the $\alpha,\beta,\gamma,\delta$-unsaturated carbonyl. This carbonyl was assigned as a primary amide on the basis of the molecular formula, but conclusive evidence could not be obtained from the IR spectrum due to the overlap of the NH vibrations for the primary or secondary amide with the OH vibrations from the secondary alcohols.

One final connection, which could not be gleaned from the available data, was required to complete the planar structure of **1**. While it was clear that the oxygen attached to C-13 was connected to the ketal carbon C-16, there were no other HMBC correlations that indicated whether the second oxygen atom of the ketal was attached to C-7, C-9, or C-11. Several strategies that could have potentially resolved this issue were considered. These strategies included re-recording the gHMBC spectra under conditions where the 90° pulses, delay values, and $^3J_{CH}$ coupling constants had been optimized for the protons and carbons of interest, re-recording the COSY data in solvents such as DMSO or pyridine, where the exchangeable proton would likely be visible, acylation of the secondary alcohols, or using the β-isotope effect. Due to its operational simplicity, the potential of the latter was evaluated. To this end, a carbon spectrum of compound **1** was acquired in a 1:1 mixture of CD_3OD and CD_3OH. Carbons that were β to an exchangeable proton, i.e., a carbinol, are doubled. This is due to the sample existing as an equilibrium mixture of hydrogen-bearing and deuterium-bearing hydroxyl groups, where the substitution of the heavier isotope causes a change in the chemical shift of the β-carbon due to changes in the potential energy and bond distance (Figure 2).[16] On the basis of this carbon spectrum, hydroxyl groups were clearly attached to C-7 (δ_C 75.8 and 75.5) and C-9 (δ_C 78.1 and 78.0), and therefore, the oxygen atom attached to C-16 was joined to C-11 to form the 1,4-dimethyl-2,8-dioxabicyclo[3.2.1]-octan-3-yl ring system.

Concurrently, examination of another strain of *S. arenicola* isolated from a sediment sample collected in Guam at a depth of 300 m led to the identification of a more polar analogue, salinikeltal B (**2**). This compound analyzed for the molecular formula $C_{22}H_{37}NO_6$ on the basis of a pseudomolecular ion peak at 434.2516 ([MH]$^+$, error 0.6 ppm) that indicated **2** contained the same number of degrees of unsaturation as **1**. Likewise, the NMR spectra of the two compounds were nearly superimposable, except for the absence of signals for the allylic methyl in the NMR spectrum of **2** and the presence of a new oxygenated methylene carbon signal at δ_C 65.1. These data suggested **2** was the 18-hydroxyl analogue of **1**, which was subsequently confirmed by analysis of the 2D NMR data.

With these two planar structures in hand, we turned our attention to assigning the relative stereochemistry of **1**. A variety of

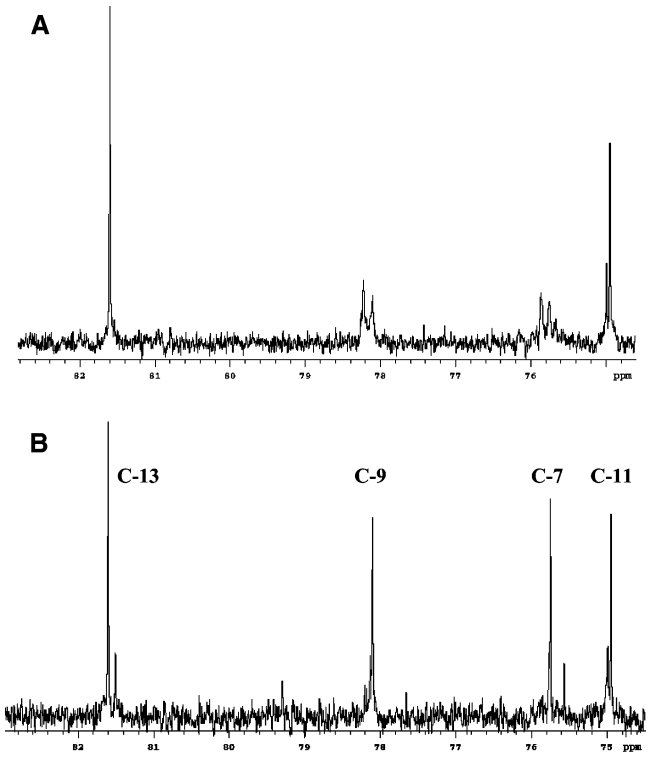

Figure 2. ^{13}C NMR spectrum in (A) 1:1 CD_3OD/CD_3OH and (B) CD_3OD. In the former, the carbinol carbons are broadened and doubled.

techniques were needed to accomplish this task including 1D NOE experiments and *J*-based configurational analysis. Briefly, the relative stereochemistry was assigned as follows. First, the configuration of the C-4/C-5 double bond was assigned as *E* on the basis of the H-4/H-5 proton−proton coupling constant of 15.3 Hz, while C-2/C-3 was assigned as *E* on the basis of an NOE correlation between H-3 and H_3-18. The chiral centers were assigned by applying the rules outlined by Murata et al. for conformational analysis of acyclic systems using proton−carbon coupling constants (Figure 3).[17] On the basis of the large proton−proton coupling constant of 9.3 Hz, indicative of an *anti* orientation between H-6 and H-7, the configuration of these centers could be determined by 1D NOE experiments. Irradiation of the methyl doublet at 0.96 ppm (H_3-19) gave an NOE enhancement of H-8, while irradiation of H_3-20 resulted in an observable NOE correlation to H-6. Taken together, these data established the *anti* relationship of the methyl group H_3-19 and the alcohol functionality attached to C-7. Likewise, the relative configuration between C-9 and C-10 could be established by NOE correlations due to the presence of a single rotamer between these two carbons, as indicated by the large proton−proton coupling constant of 8.3 Hz between their respective protons. In this case, NOE correlations between H_3-21 and H-8 established an *anti* relationship between the C-9 hydroxyl and the H_3-21 methyl groups.

To determine the relative stereochemistry of several of the other centers (C-7/C-8, C-8/C-9, C-10/C-11, and C-12/C-13), the two- and three-bond proton−carbon coupling constants were determined through analysis of the spectrum obtained in a gHSQMBC experiment.[18] Due to the complex multiplicity of the methine proton resonances, not all the coupling constants could be accurately determined with the amount of material on hand. Fortunately, the spectrum did have adequate signal-to-noise so that enough values could be determined to assign the relative stereochemistry of the vicinal centers C-7/C-8, C-10/C-11, and C-12/C-13, as depicted (Figure 3). However, for the reasons described before, the configuration of C-8/C-9 could not be assigned. We next attempted to assign this stereochemistry by comparing the carbon chemical shift

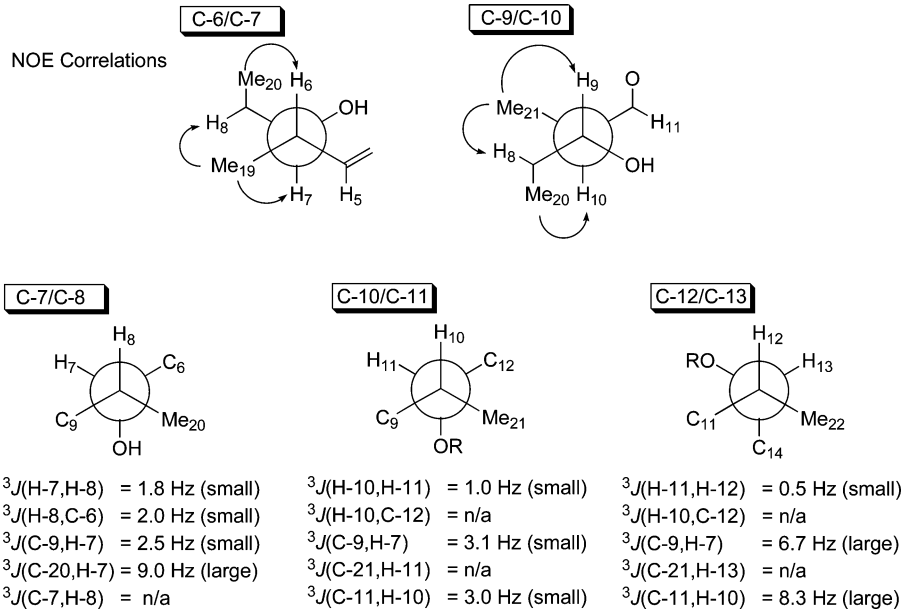

Figure 3. NOE correlations and coupling constants used to determine the relative stereochemistry of **1**. Coupling constants marked "n/a" could not be accurately assigned due to poor signal-to-noise.

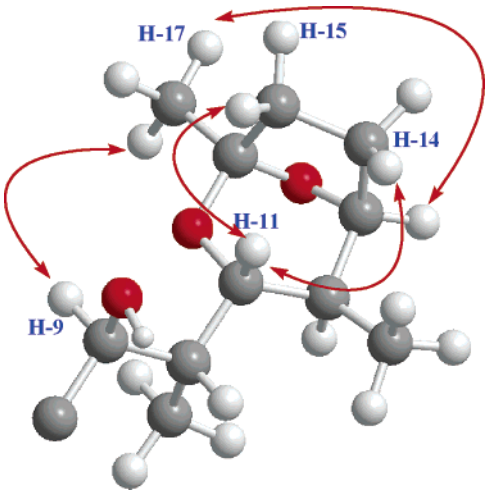

Figure 4. NOE correlations used to establish the configuration of the ring.

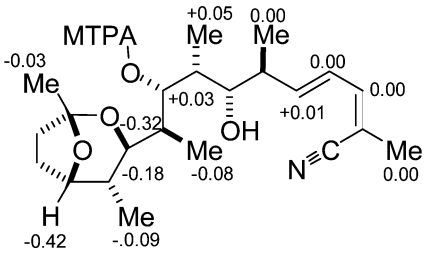

Figure 5. $\Delta\delta_{S-R}$ values (ppm) for the C-9 MTPA derivatives.

of C-20 with the literature values reported for the 2-methyl-1,3-diol in the universal NMR database.[19] Unfortunately, our value of 11.1 ppm did not allow us to discriminate between the *syn*/*anti* or *anti*/*anti* configurations (10.7 and 11.6 ppm, respectively). In the end, it became necessary to prepare an acetonide derivative of **1** to establish the stereochemistry of the 1,3-diol. The methyl carbon chemical shifts of 24.8 and 23.9 ppm in this derivative, as determined by a gHSQC experiment, established an *anti* relationship between the hydroxyl groups on C-7 and C-9.[20] Finally, NOE correlations from H-11 to H-14$_a$ and H-15$_a$ established the stereochemical configuration around the 1,4-dimethyl-2,8-dioxabicyclo-[3.2.1]octan-3-yl ring (Figure 4).

To determine the absolute configuration of **1**, the modified Mosher method was applied. When **1** was treated with an excess of α-methoxy(trifluoro)phenylacetyl chloride (MTPA-Cl) in pyridine, it resulted in the quantitative conversion to a less polar compound with a molecular weight suggestive of a dehydration product (MW 377). We initially suspected this product was formed from the loss of the C-7 hydroxyl group that would result in an extended system of conjugation that was consistent with a bathochromic shift of the UV absorption maximum. This product was then converted to the mono-MTPA derivative with (*R*)-MTPA-Cl, which reacted substantially faster than (*S*)-MTPA-Cl. Reaction with the *S* acid chloride came to completion in under 4 h, while the *R* isomer required 20 h at an elevated temperature. NMR analysis of the products indicated that C-9 had been acylated with Mosher's reagent, allowing the assignment of the absolute configuration of this center as depicted (Figure 5). Surprisingly, it also indicated that the C-7 hydroxyl group had not been lost as we originally expected on the basis of the MS data. This unexpected result seriously called into doubt our proposed structures and, thus, the validity of our Mosher analysis. Unfortunately, a complete structural assignment of these Mosher derivatives could not be made conclusively due to the limited amount of material that had been prepared. So the reaction was carried out on a larger scale (2.7 mg of **1**) using (*R*)-MTPA-Cl, which again produced the dehydration product followed by conversion, this time to the di-MTPA derivative after 16 h.[21] This product was then fully characterized by 2D NMR spectroscopic methods. The data obtained conclusively showed that the carbon backbone, including the bicyclic ring in **1**, was still intact. A closer inspection of these data revealed the site of dehydration. Specifically, the allylic methyl group no longer showed a HMBC correlation to the amide carbonyl that had been at 175.1 ppm. Instead, it showed a strong cross-peak to a quaternary carbon at 119.0 ppm, the chemical shift of which was indicative of a nitrile quaternary carbon. This functional group interconversion is surprising since, in general, this dehydration requires much more vigorous reaction conditions. In this case, the reaction is likely facilitated by the degree of conjugation of the amide that serves to increase the nucleophilicity of the carboxyl oxygen toward acylation and subsequent dehydration. To our knowledge, however, this is the first reported example of the conversion of a primary amide to a nitrile using Mosher's chloride,[22] and this result should stand as a

Table 1. NMR Spectroscopic Data for Saliniketal A (**1**) in CD_3OD

C/H no.	δ_C	δ_H (*J* Hz)	COSY	HMBC	NOESY
1	175.1, qC				
2	131.4, qC				
3	134.1, CH	6.17, br d (11.1, 1.2)	4, 18	1, 2, 4, 5, 18	4, 5, 18
4	128.3, CH	6.60, dd (15.3, 11.1)	3, 5	2, 3, 6	3, 5, 6, 19
5	142.0, CH	5.78, dd (15.3, 8.4)	4, 6	3, 6, 19	3, 4, 5, 6, 7, 19
6	42.3, CH	2.35, m (9.3, 8.4, 6.8)	5, 7, 19	4, 5, 7, 19	19, 20
7	75.8,[a] CH	3.71, dd (9.3, 1.8)	6, 8	5, 9, 20	4, 6, 8, 11, 19, 21
8	35.7, CH	1.88, m (7.4, 4.9, 1.8)	7, 9, 20	9, 20	
9	78.2,[a] CH	3.52, dd (8.3, 4.9)	8, 10	7, 21	8, 20, 21
10	37.1, CH	1.84, br dq (8.3, 7.2, 1.4)	9, 11, 21		
11	74.9, CH	3.97, br d (10.8, 1.4)	10, 12	9, 10, 13, 21, 22	9, 13, 14_d, 15_d, 20, 21, 22
12	35.2, CH	2.00, dqd (10.8, 7.3, 3.4)		13, 14	
13	81.6, CH	4.23, br dd (6.3, 3.4)	14_a	16	11, 12, 14, 22
14_a	24.9, CH_2	1.94, m		16	11
14_b		1.90, m		13	
15_a	35.1, CH_2	2.05, m		16	11
15_b		1.80, m		16, 17	
16	106.4, qC			17	
17	24.2, CH_3	1.39, s		15_a, 16	9, 11, 13
18	20.9, CH_3	1.94, d (1.2)	3	1, 2, 3	
19	17.1, CH_3	0.96, d (6.8)	6	5, 6, 7	8
20	11.1, CH_3	1.02, d (7.3)	8	7, 8, 9	7, 9, 12
21	10.2, CH_3	0.89, d (7.2)	10	9, 10, 11	7, 9
22	12.8, CH_3	0.76, d (7.3)	12	12, 13	12, 15_a

[a] These ^{13}C NMR signals are doubled in a 1:1 mixture of CD_3OH/CD_3OD.

precautionary tale when interpreting NMR data of derivatives containing primary amides.

A significant body of research devoted to ornithine decarboxylase has accumulated since the discovery of the mammalian isoform of this enzyme and its role in cell growth.[23] It is now known that ODC is present in a considerable array of species, including both prokaryotes and eukaryotes. While mammalian ODCs are highly conserved, comparisons of prokaryotic and eukaryotic ODC amino acid sequences show few similarities. Despite these structural differences, several inhibitors of ODC activity are effective against both mammalian and bacterial forms. For example, while α-difluoromethylornithine (DFMO, eflornithine) has no time-dependent effect on bacterial ODC,[24] the corresponding monofluoro derivative is active against both mammalian and bacterial ODC.[23a] These latter results suggested that bacteria might have evolved ODC inhibitors that may be effective against mammalian homologues. Saliniketals A and B were tested for potential to inhibit ornithine decarboxylase activity, but were found to be inactive at concentrations up to 1 mM (data not shown).

Interestingly, however, several other compounds derived from marine sources have been shown to induce ODC activity, including calyculin A[25] and okadaic acid from marine sponges, and lyngbyatoxin A and debromoaplysiatoxin isolated from the marine cyanobacterium *Lyngbya majuscula*.[26] Despite their structural diversity, these compounds have been shown to serve as tumor promoters. While the ecological significance of these compounds and their effect on ODC have not been fully investigated, it is interesting to note that in the case of *Vibro cholerae* a polyamine sensor has been identified that mediates biofilm formation.[27] This raises the intriguing speculation that the potential ecological role of these natural products is to regulate the formation or composition of the bacterial communities associated with sponges and cyanobacteria by either promoting or inhibiting polyamine production.[28]

Saliniketals A and B were tested for ODC induction capability using culture T24 cells as a model and found to be inactive. Conversely, however, when tested in conjunction with TPA, a potent tumor promoter that induces ODC activity, saliniketals A and B were found to weakly but significantly inhibit induction with IC_{50} values of 1.95 ± 0.37 and 7.83 ± 0.12 μg/mL, respectively.

The saliniketals are also of interest because of their structural relationship to the *ansa* side chain (C-1 through C-15 in blue) of the rifamycin structural class (**3**) of antibiotics, which co-occur within the fermentation broth. Despite the structural similarities, however, **1** does not have a significant bactericidal effect. This lack of antibacterial activity of **1** can be rationalized on the basis of the SAR data for rifamycin, which indicate that the ability of **3** to inhibit the initial phase of DNA-dependent RNA polymerase in prokaryotes is highly dependent on the formation of four key hydrogen bonds between the four free hydroxyl groups (7-OH, 9-OH, 23-OH, 25-OH) and the polymerase. Obviously, **1** lacks the two phenolic protons present in rifamycin and is therefore unlikely to form all the hydrogen bonds required for this inhibition. Elegant work with stable precursor and molecular genetics has established that the rifamycins are polyketides assembled from an aromatic starter unit, 3-amino-5-hydroxybenzoic acid, that is elaborated with two acetate and eight propionate units.[29] This suggests that saliniketals A and B are not degradation products or shunt metabolites from rifamycin biosynthesis. The presence of a primary amide in these compounds is unlikely to arise from any degradative process involving cleavage of the *ansa* side chain from the aromatic ring. Also, since the nitrogen of the amide bond in rifamycin originates from the aromatic starter unit, the presence of the primary amide in **1** implies it is most likely not a shunt metabolite of rifamycin biosynthesis. Therefore, the saliniketals appear to be formed from an unusual three-carbon starter unit, i.e., glycolate[30] or pyruvate, followed by elongation with two acetate and five propionate units, which results in a heptadecaketide with chiral centers of identical stereochemistry to those in rifamycin. The genetic significance of these similarities will be revealed once the genome sequencing of *S. arenicola* is complete.[31]

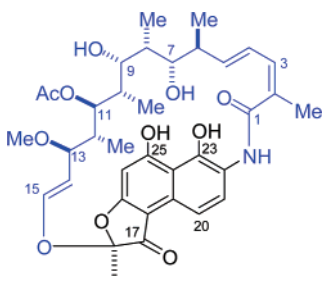

Rifamycin (**3**)

Experimental Section

General Experimental Procedures. Optical rotations were measured on an Autopol III automatic polarimeter at the sodium line (589 nm). UV spectra were obtained on a Shimadzu UV-1601 UV−visible

spectrophotometer, and IR bands were measured as a thin film on a NaCl disk using a Perkin-Elmer 1600 series FTIR. NMR spectra were acquired on a Varian Inova 500 MHz spectrometer operating at 500 or 125 MHz using the residual solvent signals as an internal reference (CD_3OD δ_H 3.30 ppm, δ_C 49.0 ppm). Low-resolution mass spectrometric data were obtained on a Hewlett-Packard 1100 series MSD, and high-resolution mass spectrometric data were measured on an Ion Spec Ultima MALDI-FTMS using the ES mode.

Fermentation. Strain CNR-005 was isolated from a sediment sample collected in Guam at a depth of approximately 30 m in January 2002. The producing organism was cultured in 40 × 1 L Fernbach flasks containing A1BFe medium (10 g of starch, 4 g of yeast extract, 2 g of peptone, 5 mL of $Fe_2(SO_4)_3 \cdot 4H_2O$ at 8 g/L, 5 mL of KBr at 20 g/L, 1 L of seawater) for 7 days at 25−27 °C while shaking at 230 rpm. Strain CNR-059 was isolated from a sediment sample collected in Guam at a depth of approximately 300 m in January 2002. It was fermented in 9 × 1 L Fernbach flasks using the same medium that was used for CNR-005 except for the addition of 1 g of $CaCO_3$ per liter of seawater. The identification of these two strains was accomplished by 16s rRNA gene analysis. Both strains are highly homologous to *Salinispora arenicola*, the systematic description of which has appeared.[31]

Isolation of Saliniketal A from CNR-005. Sterilized Amberlite XAD-16 resin (20 g) was added to each flask on day 7 and the slurry shaken for 24 h before it was filtered off from the bacterial cells and washed with water. The resin was then extracted overnight with acetone and the organic extract concentrated in vacuo to afford ca. 30 g of crude extract. This residue was separated by a silica flash column eluting with DCM, 10% MeOH in DCM, 20% MeOH, and MeOH.

The residue from the 10% MeOH fraction was separated by a reversed-phase (RP) flash column eluting with 25, 50, 75, and 100% CH_3CN in water. The residue from the 50% fraction was separated by RP HPLC (Ultracarb C_{18}, 10 × 250 mm, 2.5 mL/min; ELSD detection, 25% CH_3CN in water for 10 min then a linear gradient up to 100% over 50 more min) to afford saliniketal A (**1**) (ca. 20 mg; t_R = 32 min).

Isolation of Saliniketals A and B from CNR-059. The crude extract (6 g from 9 L) was generated from the fermentation broth as described above. This extract was separated by a RP flash column eluting sequentially with 10, 30, 45, 55, 65, 85, and 100% MeOH in water. The residue from the 65% fraction was separated by RP HPLC (Waters Prep, LC 4000 system, Waters preparative column C_{18} 60 Å, 25 × 200 mm, 10 mL/min; UV detection at 210 nm, 25% CH_3CN in water for 10 min and then a linear gradient up to 40% over 40 more min) to afford saliniketal B (ca. 2.2 mg; t_R = 25 min) and saliniketal A (ca. 6 mg, t_R = 37 min).

Saliniketal A (**1**, 20 mg, 0.07% yield): amorphous powder; $[\alpha]_D$ −13.7 (*c* 0.133, MeOH); UV (MeOH) λ_{max} (log ϵ) 240 (3.1) nm; IR (NaCl) ν_{max} 3354, 3201, 1719, 1660, 1598, 1454, 1384, 1331, and 1014 cm^{-1}; ^1H and ^{13}C NMR data (CD_3OD), see Table 1; ESIMS *m*/*z* 418 $(M + Na)^+$; HRMALDI-FTMS *m*/*z* 396.2760 [calcd for $C_{22}H_{38}NO_5^+$, 396.2750].

Saliniketal B (**2**, 2.2 mg, 0.03% yield): amorphous powder; $[\alpha]_D$ −22.4 (*c* 0.107, MeOH); UV (MeOH) λ_{max} (log ϵ) 242 (4.0) nm; IR (NaCl) ν_{max} 3350, 3198, 1720, 1664, 1604, 1460, 1384, 1184 cm^{-1}; ^1H and ^{13}C NMR data (CD_3OD), see Table S1; ESIMS *m*/*z* 434 $(M + Na)^+$; HRESITOFMS *m*/*z* 434.2516 [calcd for $C_{22}H_{37}NO_6Na^+$, 434.2513].

Acknowledgment. We thank the National Cancer Institute, NIH, for research support through grant P01 CA48112 and the NIH Shared Resources Program for instrumentation funded by grant S10RR017768. Additional financial support was provided by the University of California Industry-University Cooperative Research Program (IUCRP, grant BioSTAR 10354). P.R.J. and W.F. are scientific advisors to and stockholders in Nereus Pharmaceuticals, the corporate sponsor of the IUCRP award. The terms of this arrangement have been reviewed and approved by the University of California, San Diego, in accordance with its conflict of interest policies. High-resolution mass spectrometric analyses were carried out by the UCR Mass Spectrometry Facility, Department of Chemistry, University of California, Riverside. We thank L. Zeigler and C. Kauffman, SIO, for assistance with bioassays and fermentation. We thank W. Yoshida of the University of Hawaii at Manoa and T. Bugni of the University of Utah, Salt Lake City, for assistance with the gHSQMBC experiment.

Supporting Information Available: Complete synthetic procedures for the formation of the derivatives and for the assay protocol and tabulated NMR data for **2** together with ^1H, ^{13}C, gCOSY, gHMBC, and gHSQC NMR spectra for **1** and **2**. This material is available free of charge via the Internet at http://pubs.acs.org.

References and Notes

(1) Ries, L. A. G., Eisner, M. P., Kosary, C. L., Hankey, B. F., Miller, B. A., Clegg, L., Mariotto, A., Feuer, E. J., Edwards, B. K., Eds. SEER Cancer Statistics Review, 1975−2002, National Cancer Institute: Bethesda, MD, http://seer.cancer.gov/csr/1975_2002/, based on November 2004 SEER data submission, posted to the SEER web site 2005.
(2) Hong, W. K.; Sporn, M. B. *Science* **1997**, *275*, 1073−1077.
(3) Lee, S. K.; Luyengi, L.; Gerhäuser, C.; Mar, W.; Lee, K.; Mehta, R. G.; Kinghorn, D.; Pezzuto, J. M. *Cancer Lett.* **1999**, *136*, 59−65.
(4) Tabor, H.; Hafner, E. W.; Tabor, C. W. *J. Bacteriol.* **1980**, *144*, 952−956.
(5) Tabor, C. W.; Tabor, H.; Tyagi, A. K.; Cohn, M. S. *Fed. Proc.* **1982**, *41*, 3084−3088.
(6) Pendeville, H.; Carpino, N.; Marine, J.-C.; Takahashi, Y.; Muller, M.; Martial, J. A.; Cleveland, J. L. *Mol. Cell. Biol.* **2001**, *21*, 6549−6558.
(7) Chang, Z. F.; Chem, K. Y. *J. Biol. Chem.* **1988**, *263*, 11431−11435.
(8) Gerner, E. W.; Garewal, H. S.; Emerson, S. S.; Sampliner, R. E. *Cancer Epidemiol. Biomarkers Prev.* **1994**, *3*, 325−330.
(9) Bello-Fernandez, C.; Packham, G.; Cleveland, J. L. *Proc. Natl. Acad. Sci. U.S.A.* **1993**, *90*, 7804−7808.
(10) Pena, A.; Reddy, C. D.; Wu, S.; Hickok, N. J.; Reddy, E. P.; Yumet, G.; Soprano, D. R.; Soprano, K. J. *J. Biol. Chem.* **1993**, *268*, 27277−27285.
(11) Gerner, E. W.; Meysken, F. L., Jr. *Nat. Rev. Cancer* **2004**, *4*, 774−792.
(12) Kelloff, G. J.; Boone, C. W.; Crowell, J. A.; Steele, V. E.; Lubet, R. A.; Siman, C. S. *Cancer Epidem. Biomarkers Prevent.* **1994**, *3*, 83−98.
(13) Szarka, C. E.; Grana, G.; Engstrom, P. *Curr. Probl. Cancer* **1994**, *18*, 1−78.
(14) Lee, S. K.; Pezzuto, J. M. *Arch. Pharmacol. Res.* **1999**, *22*, 559−564.
(15) Ignatenko, N. A.; Zhang, H.; Watts, G. S.; Skwan, B. A.; Stringer, D. E.; Gerner, E. W. *Mol. Carcinog.* **2004**, *39*, 221−233.
(16) Breitmaier, E.; Voelter, W. *Carbon-13 NMR Spectroscopy*; VCH: Germany, 1987, p 117.
(17) Matsumori, N.; Kaneno, D.; Murata, M.; Nakamura, H.; Tachibana, K. *J. Org. Chem.* **1999**, *64*, 866−876.
(18) Williamson, R. T.; Marquez, B. L.; Martin, G. E.; Krishanmurthy, V. V.; Gerwick, W. H.; Koehn, F. E. *Magn. Reson. Chem.* **2001**, *39*, 544−548.
(19) Kobayashi, Y.; Tan, C.-H.; Kishi, Y. *J. Am. Chem. Soc.* **2001**, *123*, 2076−2078.
(20) Rychnovsky, S. D.; Rogers, B.; Yang, G. *J. Org. Chem.* **1993**, *58*, 3511−3515.
(21) The di-MTPA derivative was produced in this case to conclusively establish the presence of the hydroxyl groups at C-7 and C-9.
(22) Pivaloyl chloride has been recently shown to convert primary amides to nitriles. See: Narsaiah, V. A.; Nagaiah, K. *Adv. Synth. Catal.* **2004**, *346*, 1271−1274.
(23) For reviews on ODC as a drug target see: (a) McCann, P. P.; Pegg, A. E. *Pharmac. Ther.* **1992**, *54*, 195−215. (b) Herby, O.; Roberts, S. C.; Ullman, B. *Biochem. Soc. Trans.* **2003**, *31*, 415−419.
(24) (a) Bey, P.; Danzin, C.; Jung, M. Inhibition of basic amino acid decarboxylases involved in polyamine biosynthesis. In *Inhibition of Polyamine Metabolism. Biological Significance and Basis for New Therapies*; McCann, P. P., Pegg, A. E., Sjoerdsma, A.. Eds.; Academic Press: Orlando, 1987; pp 1−32. (b) Kallio, A.; McCann, P. P. *Biochem. J.* **1981**, *200*, 69−75.
(25) Suganuma, M.; Fujiki, H.; Furuya-Suguri, H.; Yoshizawa, S.; Yasumoto, S.; Kato, Y.; Fusetani, N.; Sugimura, T. *Cancer Res.* **1990**, *50*, 3521−3525.
(26) Fujiki, H.; Mori, M.; Nakayasu, M.; Terada, M.; Sugimura, T.; Moore, R. E. *Proc. Natl. Acad. Sci. U.S.A.* **1981**, *78*, 3872−3876.
(27) Karatan, E.; Duncan, T. R.; Watnick, P. I. *J. Bacteriol.* **2005**, *187*, 7434−7443.
(28) To the best of our knowledge it is not known if okadaic acid, lyngbyatoxin A, or debromoaplysiatoxin has any effect on bacterial ornithine decarboxylases.

(29) Floss, H.; Yu, T.-W. *Chem. Rev.* **2005**, *105*, 621−632.
(30) Feeding studies have shown glycolate to be the starter unit in several natural products. For a review see: Moore, B. S.; Hertweck, C. *Nat. Prod. Rep.* **2002**, *19*, 70−99.
(31) A rough draft of the *S. arenicola* genome has been obtained and is currently being analyzed. These results will be disclosed elsewhere.
(32) Udeani, G. O.; Gerhäuser, C.; Thomas, C. F.; Moon, R. C.; Kosmeder, J. W.; Kinghorn, A. D.; Moriarty, R. M.; Pezzuto, J. M. *Cancer Res.* **1997**, *57*, 3424−3428.
(33) Gills, J.; Jeffery, E. H.; Matusheski, N. V.; Moon, R. C.; Lantvit, D. D.; Pezzuto J. M. *Cancer Lett.* **2005**, *236*, 72−79.

NP0604580